

# UC Irvine

## UC Irvine Previously Published Works

### Title

Measurements of the neutron source strength at DIII-D

### Permalink

<https://escholarship.org/uc/item/9rg9c8w3>

### Journal

Review of Scientific Instruments, 68(1)

### ISSN

0034-6748

### Authors

Heidbrink, WW  
Taylor, PL  
Phillips, JA

### Publication Date

1997

### DOI

10.1063/1.1147646

### Copyright Information

This work is made available under the terms of a Creative Commons Attribution License, available at <https://creativecommons.org/licenses/by/4.0/>

Peer reviewed

# Measurements of the neutron source strength at DIII-D

W. W. Heidbrink

University of California, Irvine, California 92717

P. L. Taylor

General Atomics, San Diego, California 92138

J. A. Phillips

University of California, Irvine, California 92717

(Presented on 14 May 1996)

A set of neutron counters and a pair of scintillators measure the 2.5 MeV neutron emission produced by the DIII-D tokamak. The neutron counter set provides a large dynamic range ( $\sim 7$  orders of magnitude) while the scintillators provide the very fast resolution needed for studying transient events. The counters are absolutely calibrated *in situ* with a  $^{252}\text{Cf}$  source and the scintillators are cross calibrated to the counters. The historic variations in the emission measured by the various detectors have been compared and are consistent within the estimated accuracy of the absolute calibration (15%). In the discharges with the highest emission levels ( $2.4 \times 10^{16}$  n/s), the signals from the neutron counters and the scintillators agree well. Comparisons with other diagnostics also corroborate the neutron measurements. © 1997 American Institute of Physics.

[S0034-6748(97)56401-X]

## I. INTRODUCTION

For the last decade, counters<sup>1,2</sup> and scintillators<sup>3,4</sup> have measured the 2.5 MeV neutron emission produced by DIII-D. Recently, emission in excess of  $2 \times 10^{16}$  n/s in the relatively modest DIII-D tokamak<sup>5</sup> has focused attention on the accuracy of the neutron measurements. This article documents the calibration procedure and describes several tests of the validity of the measurements.

## II. DETECTORS AND CALIBRATION

The two neutron diagnostic systems are conventional. The epithermal counters consist of four moderators. Three of the moderators use lead and paraffin shields and have five proportional counters (one  $^3\text{He}$  detector and four  $\text{BF}_3$  detectors) while the fourth moderator has a polyethylene shield and three  $^{235}\text{U}$  fission counters. A range of sensitivities is achieved by using detectors of different sizes and amounts of active material, and by wrapping some detectors in cadmium foil. The moderators are situated at different toroidal locations, 4 to 7 m radially from the center of the machine, near the horizontal midplane. Standard pulse-counting electronics (preamplifiers, amplifiers, scalars, and digitizers) are employed.

The neutron scintillators are similar to the system employed on PDX and TFTR.<sup>6</sup> A 5-in.-diam plastic scintillator (Bicron BC-400) is mounted between toroidal field coils just outside a 1-in.-thick stainless-steel flange. The detector, mounted vertically off axis, views the center of the plasma at an angle of  $45^\circ$  to the midplane of the machine. A  $\text{ZnS}(\text{}^6\text{Li})$  scintillator is mounted underneath the plastic scintillator behind a 2-in.-thick acrylic moderator. Both scintillators employ 2-in.-diam acrylic rods as light guides. Approximately 3 m from the vessel, the light guides connect to shielded photomultiplier tubes (PMTs). The gain of the photomultipliers is controlled by remote high voltage power sup-

plies; the output is measured in current mode using a preamplifier and transient digitizers.

The neutron counters have a dynamic range between  $10^9$  and  $10^{17}$  neutrons/s with a maximum time resolution of 10 ms. The scintillators are useful when the source strength exceeds  $\sim 10^{11}$  n/s. The frequency response of the plastic scintillator is  $\sim 100$  kHz, while the  $\text{ZnS}$  scintillator has a response of  $\sim 5$  kHz.

The plastic scintillator is more sensitive to hard x rays produced by runaway electrons than the other detectors.<sup>6</sup> In practice, x-ray contamination of the signal is only rarely observed (e.g., during unusual disruptions or during operation with electron density  $\bar{n}_e \lesssim 5 \times 10^{18} \text{ m}^{-3}$ ).

The absolute calibration follows a standard procedure.<sup>2</sup> At the conclusion of each major vent, a  $^{252}\text{Cf}$  source ( $10^7$  neutrons/s) is mounted on a model train situated at the magnetic axis. Translation of the source around the track simulates a toroidal line source and is used to calibrate the most sensitive detectors. To reduce uncertainties associated with counting statistics to negligible levels ( $\sim 2\%$ ), data are typically acquired for 2 h. The detectors with intermediate sensitivity are cross calibrated to the most sensitive detectors by placing the source on the moderators. (Direct calibration with the train or cross calibration during plasma discharges gives equivalent calibration factors within statistical uncertainties.) A neutron transport code<sup>1</sup> that models the DIII-D machine and the detector and its moderator computes the difference in detection efficiency for D-D neutrons relative to the  $^{252}\text{Cf}$  source; this results in a 12% correction to the measured efficiency. After each vent, plasma discharges are used to cross calibrate the least sensitive counters to the absolutely calibrated counters.

The contributions of the various uncertainties in the calibration are similar to those in Table II of Ref. 2. We compared the scintillator signals with the counter signals for a set of discharges with major radii  $R$  between 1.70 and 1.84 m;

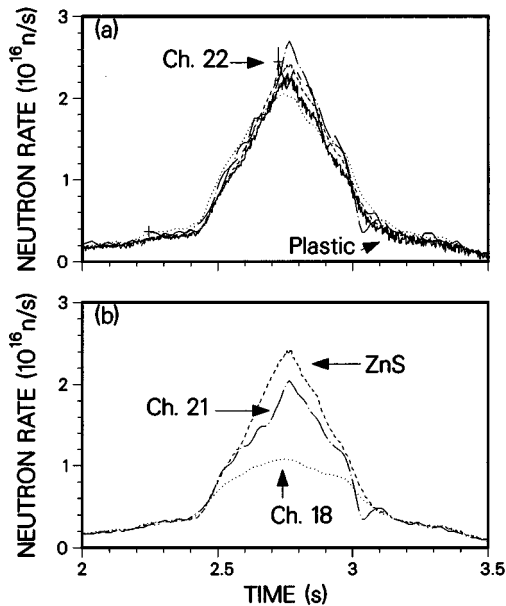


FIG. 1. Time evolution of the signals from the two scintillators and the three least sensitive counters in discharge No. 87980. The plastic (solid) and ZnS (dash) scintillator calibrations include a correction for radiation damage [Eq. (1)]. (a) With pulse-pileup correction for channel 18 (dot) and channel 21 (chain dot). The error bars represent typical counting statistics for counter channel 22 (chain dash). (b) Without pulse-pileup correction for channel 18 and channel 21.

no correlation of detection efficiency with  $R$  is observed, indicating that the sensitivity of the calibration to variations in plasma position is  $\leq 10\%$ . Overall, the uncertainty in the absolute calibration is  $\sim 15\%$  (one sigma).

To provide an independent check on the stability of the calibration, the calibrations of the scintillators are separately maintained. A single cross calibration to the counters was performed in August 1995. Light-emitting diodes (LED) are used to measure the dependence of PMT gain on bias voltage for each of the scintillators. The scintillator calibration combines three factors: the August 1995 cross calibration, the PMT gain, and a factor that corrects for gradual darkening of the optical components. (This darkening factor is not included in the data of Fig. 2.) For a given discharge, these factors contribute uncertainties of 15%,  $\sim 10\%$ , and  $\sim 5\%$  to the  $\sim 20\%$  uncertainty in the absolute calibration. On the other hand, when the PMT bias voltage is kept constant for a sequence of discharges, the *relative* uncertainty is determined by the detector noise, which can be as small as  $\sim 1\%$ .

In practice, virtually all relative measurements on DIII-D use the scintillators, while nearly all absolute measurements rely on the counters.

### III. DETECTOR COMPARISONS

Figure 1 compares the two scintillator signals with the three least-sensitive counter signals (channels 18, 21, and 22) for the discharge with the highest emission level obtained on DIII-D.<sup>5</sup> Within counting statistics, the signal from channel 22 is consistent with the signal from the ZnS scintillator. The signal from the plastic scintillator is  $\sim 10\%$  smaller. At the peak value of the neutron emission, pulse pile up has a

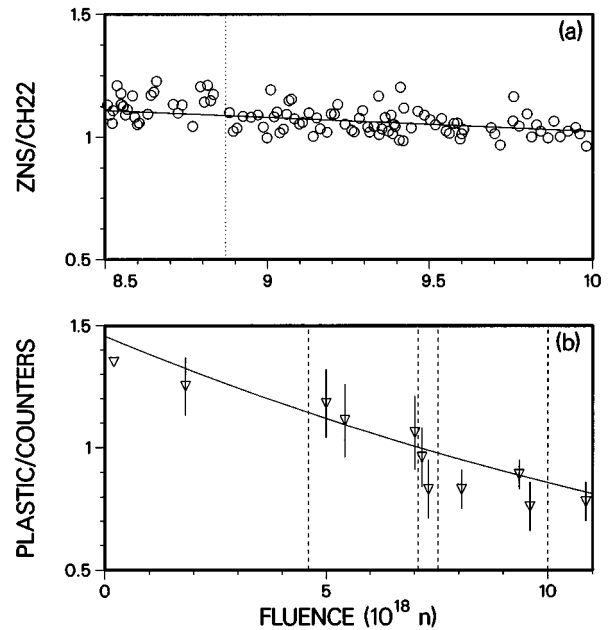


FIG. 2. (a) Ratio of the fluence measured by the ZnS scintillator to the fluence measured by the least-sensitive counter for a sequence of high-performance discharges. The abscissa represents the total fluence produced by the machine. Uncertainties associated with counting statistics are  $\leq 3\%$  for the shots in this sequence and the PMT gain was only changed once (dotted vertical line). (b) Average value (triangles) and standard deviation (error bars) of the ratio of plastic scintillator signal to counter signal for several sets of discharges. Most data points include comparisons to more than one counter channel. The abscissa represents the total fluence over the two-year period; counter recalibrations occurred at each dashed line. The solid lines in (a) and (b) show the expected behavior if the scintillator sensitivity decays exponentially with a decay constant of  $5.3 \times 10^{-20}/n$ .

strong effect on the signals from counter channels 18 and 21 [Fig. 1(b)]. A correction using the nonparalyzable model,<sup>7</sup>  $n = m / (1 - m\tau)$ , brings these signals into good agreement with the other signals [Fig. 1(a)]. (Here,  $n$  is the true interaction rate,  $m$  is the recorded count rate, and  $\tau$  is the system dead time.) This model also reconciles the data in other discharges. The value of dead time which fits the data best ( $\tau = 5 \mu\text{s}$ ) is larger than the measured FWHM of the amplifier pulse ( $1.8 \mu\text{s}$ ), presumably because there are several low-amplitude pulses (that are below the discrimination level) per counted pulse. The agreement between signals shown in Fig. 1(a) is typical.

Apart from pulse pileup effects, excellent linearity between detectors is observed. [This is apparent in Fig. 1(a).] As a discharge evolves, ratios of detector signals remain constant in time (within statistical uncertainties). As an additional check of detector linearity, ratios of detector fluences were studied for a sequence of discharges with peak emission levels that varied between  $0.8 - 8.0 \times 10^{15}$  n/s: no correlation with emission level was observed.

To assess the stability of the calibration, data acquired over a period of years are compared (Fig. 2). Relative to the counters, both scintillators gradually deteriorate in sensitivity. This trend is attributed to radiation damage in the scintillator optics. This interpretation is consistent with the observation that the calibration signals produced by the scintillator LEDs have gradually decreased over the years.

The deterioration can be modelled as exponential decay of the form

$$I \propto \exp - a\Phi, \quad (1)$$

where  $\Phi$  is the total neutron fluence produced by the machine and  $a$  is a decay constant. A decay constant of  $a = 5.3 \times 10^{-20}/n$  is consistent with the data from both scintillators (Fig. 2). Rough estimates indicate that either darkening of the acrylic light pipes or darkening of the glass PMT faceplates can account for the gradual deterioration.

The counters are recalibrated after every major vent. Changes in calibration factor of 15% for the least sensitive counters are typical. Although random errors incurred in the calibration can contribute to these variations, part of the change is caused by actual changes in detection efficiency associated with ongoing DIII-D construction. In contrast, the plastic scintillator signal is thought to be dominated by virgin (unscattered) neutrons,<sup>8</sup> so its calibration factor is unlikely to change appreciably during a major vent. Hence, comparison of the plastic signal to the counter signals before and after a vent provides an independent check on the validity of the recalibration. As shown in Fig. 2(b), no evidence of discontinuities in the counter calibration are observed at major vents.

Although agreement between detectors at the 10%–15% level is generally observed, some discrepancies remain unexplained. Figure 2(a) shows the ratio of the fluence measured by the ZnS scintillator to the fluence measured by counter channel 22 for a series of high-performance discharges (including the discharge shown in Fig. 1). For the latter portion of this sequence, the PMT bias for the ZnS scintillator was kept constant and the signal level is large, so random errors in the fluence measured by ZnS should be negligible. The expected random error for channel 22 due to counting statistics is  $\leq 3\%$  for the discharges in this sequence. Nevertheless, the observed variance for the 64 discharges in this sequence is 8%, which significantly exceeds the expected  $\sim 3\%$  variation. For other discharge conditions, comparisons between detectors reveal discrepancies considerably larger than those shown in Fig. 1. Unexplained  $\sim 20\%$  systematic discrepancies between detectors are sometimes observed.

#### IV. COMPARISON WITH OTHER DIAGNOSTICS

As a final check of the validity of the neutron measurement, we search for systematic discrepancies between the neutron measurements and the expected neutron emission. No systematic disagreements with other diagnostic measurements are found.

A simple zero-dimensional code that uses central plasma parameters to predict the neutron emission is employed. The code resembles “test particle” calculations performed by Strachan.<sup>9,10</sup> It uses central values of electron density and temperature measured by Thomson scattering,<sup>11</sup> ion temperature  $T_i$  (from the four central tangential channels), and central toroidal rotation speed  $v_{\text{rot}}$  as measured by charge-exchange recombination (CER) spectroscopy<sup>12</sup> and the injected neutral beam voltage  $W_b$  and power  $P_b$  as input parameters. Deuterium depletion and beam-beam reactions

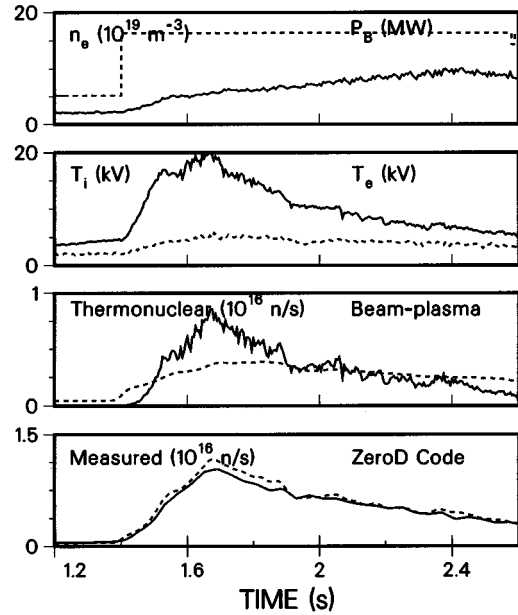


FIG. 3. Comparison of the measured neutron emission with the prediction of the zero-dimensional code for an H-mode discharge with negative central shear,<sup>16</sup> (discharge No. 87335). Electron density at  $r/a=0.3$  (solid) and beam power (dash); ion temperature inferred by averaging the four central tangential CER chords as analyzed by a neural net<sup>13</sup> (solid) and electron temperature at  $r/a=0.3$  (dash); calculated thermonuclear (solid) and beam-plasma (dash) emission; measured neutron emission (solid) and emission predicted by the zero-dimensional code (dash).

are neglected. Expressions for the D-D cross section and reactivity are taken from Bosch and Hale.<sup>14</sup> The beam-plasma reactivity is approximated as  $\langle \sigma v \rangle = (1 + c_1 T_i / W_b) \sigma v (u_{\text{eff}})$ . Here the effective directed velocity of the beam ions  $u_{\text{eff}}$  is reduced from the injection speed  $v_b$  by a factor of  $[0.6 + (0.63 - v_{\text{rot}}/v_b)^2]$  for DIII-D injection geometry, and finite ion temperature increases the reactivity by  $c_1 \approx 6.4$  for  $W_b = 75$  kV. The number of beam ions is inferred from the beam power and the slowing down time using Eq. (6) of Ref. 15.

Originally, the code had two free parameters (the coefficients for the beam-plasma rate and for the thermonuclear rate). A handful of discharges with weak magnetohydrodynamics MHDs activity were used to fit these parameters. The resulting beam target and thermonuclear coefficients are 34% and 40% higher than the coefficients used by Strachan.<sup>10</sup> Once established, no further adjustments of the coefficients were allowed in the subsequent analysis of the data.

The agreement between the zero-dimensional prediction and the measured neutron emission is often excellent. Figure 3 shows an example from a discharge with  $\sim 3$  times larger emission than the discharges used to benchmark the code. The code prediction agrees well with the measured neutron emission throughout all phases of the discharge.

To search for systematic discrepancies, a database of  $\sim 130$  discharges from the 1995 campaigns was compiled. Since Alfvén instabilities cause anomalous reductions in neutron emission,<sup>15</sup> discharges with Alfvén activity were excluded. (The availability of fast magnetics data was the principal selection criterion for the database.) For this data set,

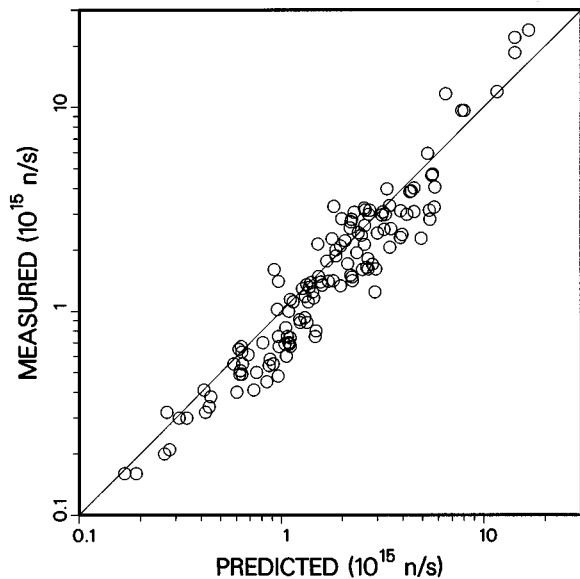


FIG. 4. Measured neutron emission (neutron counters) vs emission predicted by the zero-dimensional code. The correlation coefficient for this dataset is  $r^2=0.91$ .

the dominant scaling of the neutron emission with density, temperature, and beam voltage and power is well described by the classical predictions of the zero-dimensional model (Fig. 4). Treating the data as an ensemble, the ratio of the measured emission to the predicted emission is  $0.88 \pm 0.26$ . Presumably both measurement errors and the crude approximations of the zero-dimensional model contribute to the scatter in the data. Nevertheless, no residual dependencies on density, electron temperature, ion temperature, beam voltage,

or beam power are observed (correlation coefficient  $r^2 \leq 0.1$ ). This indicates that, to within the accuracy of the comparison, the neutron measurements are consistent with the independent measurements of  $n_e$ ,  $T_e$ , and  $T_i$ .

In conclusion, the absolute magnitude of the neutron emission is measured to an accuracy of  $\sim 15\%$  on DIII-D.

## ACKNOWLEDGMENTS

The contributions of the DIII-D team are gratefully acknowledged. This work was supported by Subcontract No. SC-L134501 of U. S. Department of Energy Contract No. DE-AC03-89ER51114.

- <sup>1</sup>Jinchoon Kim, J. K. Boshoven, R. W. Callis, J. L. Luxon, P. I. Petersen, and S. Su, in Proceedings of 13th Symposium Fusion Eng., Knoxville, 1989 (unpublished).
- <sup>2</sup>J. D. Strachan *et al.*, Rev. Sci. Instrum. **61**, 3501 (1990).
- <sup>3</sup>W. W. Heidbrink, Jinchoon Kim, and R. J. Groebner, Nucl. Fusion **28**, 1897 (1988).
- <sup>4</sup>J. A. Lovberg, W. W. Heidbrink, J. D. Strachan, and V. S. Zaveriaev, Phys. Fluids B **1**, 874 (1989).
- <sup>5</sup>E. A. Lazarus *et al.*, Phys. Rev. Lett. **77**, 2714 (1996).
- <sup>6</sup>W. W. Heidbrink, Rev. Sci. Instrum. **57**, 1769 (1986).
- <sup>7</sup>Glenn F. Knoll, *Radiation Detection and Measurement*, 2nd ed. (Wiley, New York, 1989), p. 121.
- <sup>8</sup>R. Kaita *et al.*, Nucl. Fusion **26**, 863 (1986).
- <sup>9</sup>J. D. Strachan *et al.*, Nucl. Fusion **21**, 67 (1981).
- <sup>10</sup>J. D. Strachan *et al.*, Nucl. Fusion **33**, 991 (1993).
- <sup>11</sup>T. N. Carlstrom *et al.*, Rev. Sci. Instrum. **63**, 4901 (1992).
- <sup>12</sup>P. Gohil, K. H. Burrell, R. J. Groebner, and R. P. Seraydarian, Rev. Sci. Instrum. **61**, 2949 (1990).
- <sup>13</sup>D. R. Baker, R. J. Groebner, and K. H. Burrell, Plasma Phys. Control. Fusion **36**, 109 (1994).
- <sup>14</sup>H.-S. Bosch and G. M. Hale, Nucl. Fusion **32**, 611 (1992).
- <sup>15</sup>H. H. Duong *et al.*, Nucl. Fusion **33**, 749 (1993).
- <sup>16</sup>E. J. Strait *et al.*, Phys. Rev. Lett. **75**, 4421 (1995).